Journal of the Korean Nuclear Society
Volume 27, Number 3, June 1995

Heat Transfer in the Passive Containment Cooling System

Jong Hee Cha, Hyung Gil Jun, and Moon Ki Chung
Korea Atomic Energy Research Institute
(Received August 16, 1994)

수동형 격납용기 냉각계통에서의 열전달

차종희 · 전형길 · 정문기
한국원자력연구소
(1994. 8. 16 접수)

Abstract

The objective of this work is to obtain the experimental data for the heat transfer processes occurring both on the inside and outside surfaces of containment steel wall with dry and wet outer surface conditions in the passive containment cooling system. The test model represented a 60° section of a containment vessel based on the AP 600 geometry. Major linear dimensions of the test model were reduced by a factor of ten. To simulate the decay heat, a steam generator heated by electricity was placed in the test model. The maximum heat flux was 8.91 kW/m^2. Two types of tests were performed. The one was the test on the natural convection of air without water film flow. The other was the evaporative heat transfer test with the falling water film flow and natural air draft. The test result showed that the heat transfer capability by the natural convection from the containment to the air without water film flow was limited at about 1.48 kW/m^2 heat flux. It was found that the heat removal capability was remarkably enhanced in the tests with the water film flow and air draft. The obtained heat transfer data were compared with the existing correlations.

요 약

이 연구의 목적은 수동형 격납용기 냉각계통의 용기 바깥표면이 건조 및 습한 조건일때 격납용기 내, 외벽에서 일어나는 열전달과정에 대한 실험적 자료를 얻는데 있다. 시험모델은 AP 600 구조에 근거하여 격납용기의 둘레중 60° 부분만을 취하였다. 시험모델의 주요치수는 원형의 값을 대략 10분의 1로 축소한 것이다. 붕괴열을 모의하기 위하여 전기적으로 가열되는 증기발생기를 시험모델내에 설치하였다. 최대열유속은 8.91 kW/m^2 이었다. 두 가지 형식의 시험이 수행되었다. 하나는 수막유동없이 공기만의 자연대류에 관한 시험이고 다른 하나는 수막유동과 공기의 자연대류가 동반된 증발열전달 시험이다. 시험결과 수막유동이 없는 경우 공기만의 자연대류 열전달 능력은 약 1.48 kW/m^2 열유속에서 제한되고 있음을 알게 되었다. 또한 수막유동과 공기의 자연대류가 동시에 일어나는 시험에서 열제거 능력은 현저히 향상됨을 알게 되었다. 이들 열전달 측정치들을 기존 관계식들과 비교하였다.

1. Introduction

To improve the reliability and safety of nuclear power plants, the passive concepts have been employed for several advanced reactors. The passive containment cooling system (PCCS) is one of the key passive features in advanced reactors such as the New Production Reactor, the Advanced Neutron Source, and the AP 600 for decay heat removal. In the passive containment cooling system of the AP 600[1], designed by Westinghouse, the decay heat generated in the core is removed by a series of heat transfer mechanisms which are composed with the water pool boiling in the core, condensation at the inner wall of the containment, conduction in the containment wall, and natural convection by air and/or evaporation of a falling water film at the outside of the containment steel vessel. It seems that the evaporative cooling technology is original in terms of its application to the containment cooling.

Westinghouse has performed a series of tests[2] to evaluate and characterize the heat removal capabilities of the AP 600 containment vessel. These tests included the PCCS heated plate test, the small scale integrated PCCS test, and the large scale integrated PCCS test. The tests were performed to examine the behavior of the evaporative water film cooling with air draft on the outside and the steam condensation on the inside of a containment vessel. It was reported that the measured test results agreed well with some predictions for the heat transfer processes on the AP 600 PCCS. However, the details of test data were not made available to the public. The passive containment cooling system of the AP 600 reactor will require the intensive review of the heat transfer processes at the external containment wall which is cooled by a combination of downward gravity driven water flow and upward natural circulation air flow.

The objective of this work is to obtain the experimental data for the heat transfer processes occurring both on the inside and outside surfaces of the containment steel wall with dry or wet outer surface conditions in the PCCS using the test model. Specific observations of interest include the condensation heat transfer rate that occurs on the inside surface, the convective heat transfer rate with only air natural convection at the outer surface, and the convective heat transfer rate with falling water film flow and air natural convection at the outer surface.

2. Test Description

2.1. Test facility

The test facility shown in Fig. 1 was designed to simulate the AP 600 PCCS heat transfer processes occurring both on the inside and outside containment surfaces. The test facility consists of the test model, water supply system, and the instrumentation and data acquisition system.

The test model represensted a 60° section of a containment vessel based on the AP 600 geometry. Major linear dimensions of the test model were reduced from values typical of the AP 600 containment vessel by a factor of approximately ten. Linear scaling was applied for the design of the test model. Linear scaling is the commonly used method to build a scaled-down model, especially, for the observation of the steady-state heat transfer process. The scaling ratios of major parameters were determined by Carbiener's scaling law[3]. The test model consists of a 2.328m high cylindrical dome and a 1.147m high ellipsoidal dome as shown in Fig. 2. The containment wall was made of 4mm thick steel plate, and radius of the wall carvature is 1. 98m. A transparent plexiglas cover around the containment wall, having a thickness of 5mm, was used to form the air cooling annulus. Natural convective forces cause air to flow across the surface of the containment vessel with this air flow baffle. All hot parts of the test model except the containment wall plate were completely insulated by 50mm thick glass wool to minimize heat loss. To sim ulate the heating of the containment wall that would occur in an actual plant following a postulated acci-

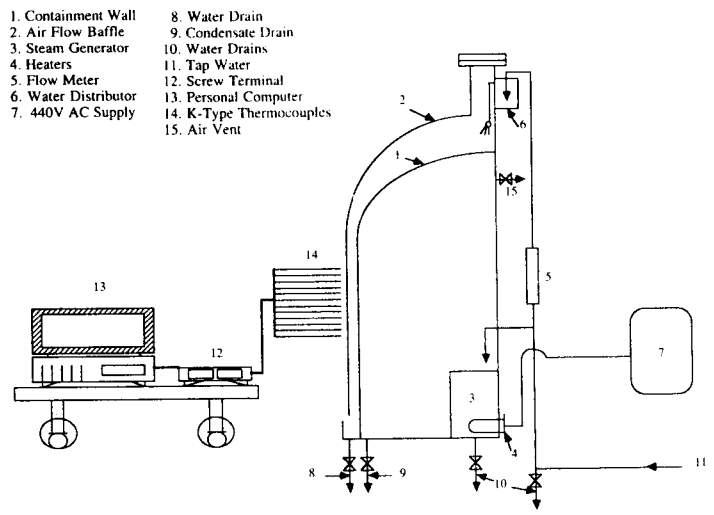

Fig. 1. Schematic Diagram of Test Facility

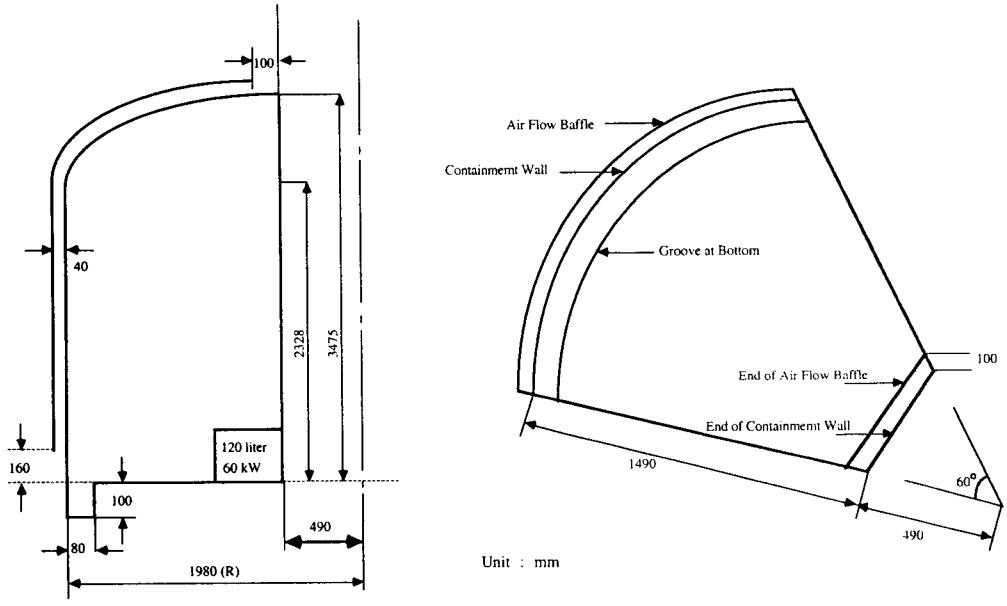

Fig. 2. Major Dimensions of Test Model

dent, a steam generator of 60 kW maximum capacity was placed in the test model.

The water supply system was divided into two ways. The one was the water supply into the steam generator, and the other was the water storage tank for cooling of the containment outer surface. Tap water was supplied to the water reservoir of the steam generator which has 120 litre water storage capacity. Steam was generated by heating with immersion heaters. Water level in the water reservoir of

the steam generator was controlled by a float valve. Another tap water line was connected with the water distributor on the top of the test model. Water was injected through the nozzles around the circular water distributor, and it flows over the containment steel surface.

The measurements of principal interest during the tests were the wall and fluid temperatures and fluid velocities in the test model. A total of 44 K-Type thermocouples were distributed on the inner and outer containment wall, and 20 thermocouples were placed at appropriate locations for the fluid temperature measurements. Fig. 3 gives an overview of the thermocouple distribution in the test model. The cooling

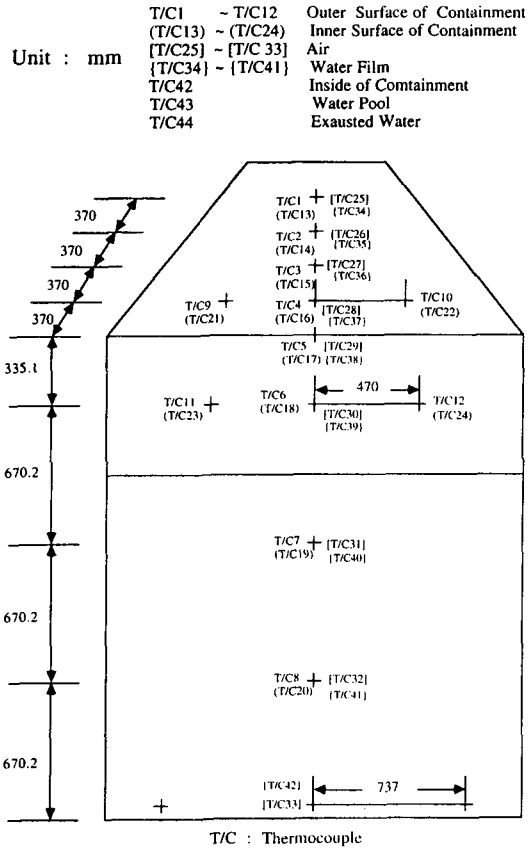

Fig. 3. Overview of Thermocouple Distribution in Test Model

air velocity was measured by conducting a velocity traverse in the cooling air annulus using a hot wire annemometer. Supplied electric power for the steam generation was measured by a watt-hour meter. Condensation rate at the containment wall was measured with the drainage rate of the condensed water. All the results of the measurements were recorded and processed on a data acquisition system.

2.2. Test Procedure

Following each test run, all valves of the test model were opened to drain water in the water reservoir of the steam generator and the bottom of the test model. After draining all valves except the air vent were closed, and water was supplied to the water reservoir of the steam generator in the test model. Electric heaters submerged in the water reservoir were turned on to heat up water. The data acquisition system was tested and prepared while water in the reservoir was heated. Steam was generated vigorously when the water temperature reached saturation state. The air vent was closed and the drain valve for drainage of the condensed water was opened when air was sufficiently evacuated by steam. As soon as the system reached a steady state, the test was started. The steady state was checked by the wall temperature and containment pressure variations as well as the drainage of the condensed water flow rate.

Following the tests with water film flow, the water was supplied from the water distributor at the top of the test model for cooling of the containment wall. The water film flow rate was increased until water film covered the whole surface of the outer wall of the test model. The water film flow rate was checked by rotameter. During the tests, the power for the steam generaton was controlled through a silicon controlled rectifier unit. The water supplied into the steam generator was automatically controlled by the float valves in the tanks.

2.3. Test Conditions

Major test parameters were the containment pressure, the water film flow rate, the steam generating power, and the temperature and humidity of the ambient air. Table 1 lists the test conditions for this work.

3. Test Results and Discussion

Heat transfer tests of the passive containment cooling were conducted using the test model under the conditions of natural convection by air with or without water film flow on the containment outer wall.

3.1. Heat Transfer with Only Air Natural Convection

Heat transfer from the outer wall of the containment to the air involves condensation of steam on the inner wall and conduction through the wall with natural convection and radiation from the outer surface of the wall to the air flow baffle. This heat is cooled by upward air natural convection inside the annulus and conduction through the air flow baffle wall and to the ambient air by natural convection and radiation. The tests were performed with varying steam generating power. Specific measured and calculated items were wall temperature transient with varying steam generating power, distribution of wall and air temperature, heat transfer coefficients at inner and outer wall, and overall heat transfer coefficients.

Table 1. Test Conditions

Parameter	Air Natural Convection without Water Film Flow	Air Natural Convection with Water Film Flow
Containment Pressure, MPa	0.1	0.1
Ambient Temperature, °C	20 ~ 24	20 ~ 24
Ambient Humidity, %	60 ~ 65	60 ~ 65
Air Flow Condition	Natural Convection (0.2~0.3 m/s)	Natural Convection (0.1~0.2 m/s)
Water Film Flow Rate, kg/s	–	0.167 0.250 0.417
Power, kW	7 ~ 30	10 20 30 40 50 60

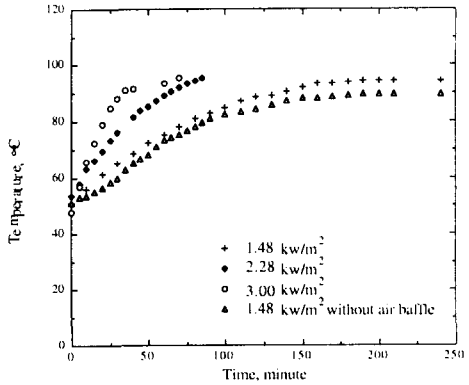

Fig. 4. Temperature Transients during Heatup under the Condition of Air Natural Convection Without Water Film Flow

Fig. 4 shows result of the measurement of the transient temperature at the specific point of the wall for the various steam generating powers. Measurement of each run was started at the time to reach the saturation temperature of water in the steam generator. In this figure, the steeper temperature rising can be found at the higher power. In the tests, the power supply system was designed so that the power could be turned off whenever containment pressure exceeded 10 percent of the atmospheric pressure. During the tests, it was observed that there was a maximum heat flux which could maintain the equilibrium state between condensation heat transfer at the inner wall

and natural convection heat transfer by air at the outer wall. The maximum heat flux, i.e., maximum cooling capability with air, was found to be 1.48 kW/m^2 in the tests. This heat flux is equivalent to the decay heat approximately 5 days after a reactor shutdown. Beyond this maximum heat flux, the containment pressure increases concurrently with heat flux due to the excess generation of steam.

Profiles of inner and outer wall temperatures and air temperatures are shown in Fig. 5. An abscissa in this figure represents the dimensionless distance from the top to the bottom along the wall, where y is any distance from the top point of the containment wall, and L is whole distance from the top to the bottom along the containment wall. The temperature differences between the inner and the outer wall are very small, and they are indicating a flat temperature distribution over the wall. The outlet air temperature closely approached the wall temperature. Measured air velocities in the air flow baffle range between 0.2 and 0.3 m/s during the tests.

Heat transfer coefficient, h, was calculated from the measurements of the wall surface temperature and the fluid temperature in the following equation:

$$h = \frac{q''}{\Delta t} \tag{1}$$

where q″ is heat flux, and Δt is temperature differenece between wall surface and fluid. In this calculation, it assumed that heat flux is uniform. The overall heat transfer coefficient, U, is defined as:

$$U = \left[\frac{1}{h_i} + \frac{t}{k} + \frac{1}{h_o}\right]^{-1} \tag{2}$$

where h_i is the heat transfer coefficient at inner wall, h_o is the heat transfer coefficient at outer wall, k is the thermal conductivity of the wall material, and t is the wall thickness.

Fig. 6 illustrates the heat transfer coefficients on the inner and outer walls, and the overall heat transfer coefficient at various locations under the heat flux condition of 1.48 kW/m^2. The values of inner wall heat transfer coefficient, i.e., the condensation heat transfer coefficients, lie within the range of 300~370 W/m^{2}K. These values are an order of magnitude lower than the values calculated from Nusselt's equation[4] for film condensation of steam. It seems that the condensation heat transfer process in this test may have been affected by air, i.e., noncondensible gas which remained in the containment atmosphere. The natural convective heat transfer coefficients with air in the annulus region ranges from 30 to 175

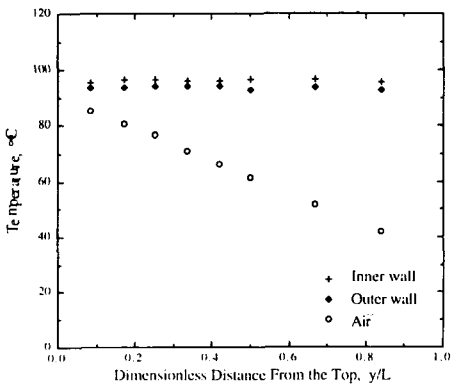

Fig. 5. Various Temperature Distributions at 1.48 kW/m^2 Heat Flux under the Condition of Air Natural Convection Without Water Film Flow

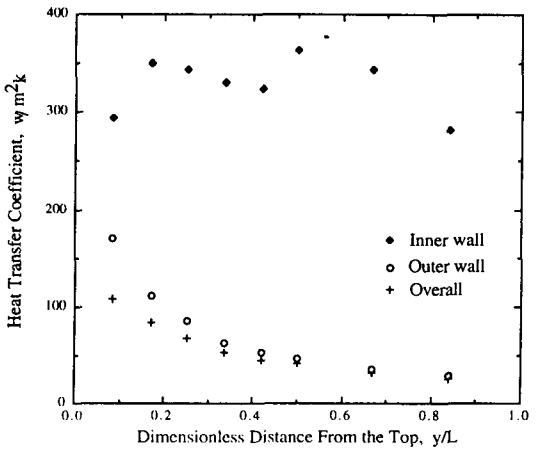

Fig. 6. Various Heat Transfer Coefficients at 1.48 kW/m^2 Heat Flux under the Condition of Air Natural Convection Without Water Film Flow

W/m^2K. As seen in this figure, the maximum heat transfer coefficient appears at the shoulder part of the containment vessel. Present data are slightly higher than Hugot's data[5] which is closely applicable to the geometry of this work as shown in Fig. 7. Shin et al. [6] have deduced in the following equation with the Hugot's data:

$$Nu = 0.108\ (GrPr)^{0.325} \quad (3)$$

where Nu is Nusselt number based on air properties and width of air flow baffle, Gr is Grashof number based on air properties, and Pr is Prandtl number of air. In Fig. 7, present data are also compared with the Churchill's correlation[7] for natural convection from a vertical plate and the modified Sparrow's correlation[8] for natural convection between two vertical cylinders.

In order to investigate the effect of the air flow baffle, a similar test was performed to demonstrate natural convection heat transfer of air without the air flow baffle. Fig. 8 shows the comparison of the heat transfer coefficients with or without the air flow baffle. In this figure, rather higher heat transfer coefficients can be found in the case of the air flow baffle removal. It seems that there is no significant effect of

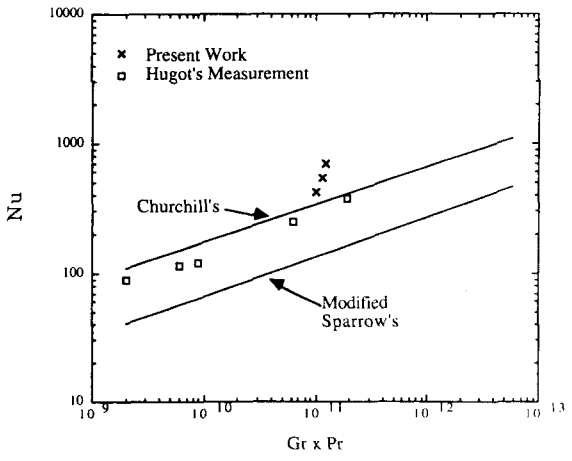

Fig. 7. Comparison of Present Data and Others for Air Natural Convection Vertical Wall

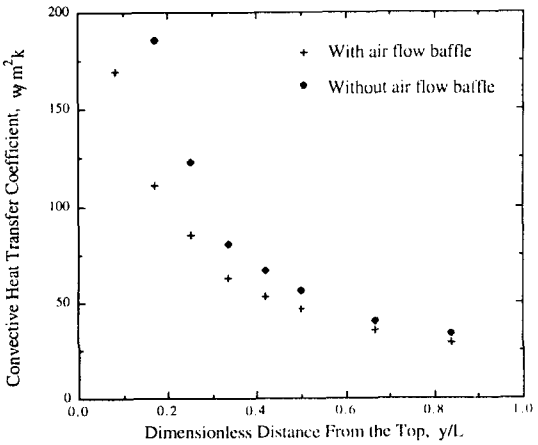

Fig. 8. Outer Wall Heat Transfer Coefficients With and Without Air Flow Baffle

the air flow baffle on air natural convection at the outer containment wall.

3.2. Heat Transfer with Water Film Flow and Air Natural Convection

Heat transfer tests of the passive containment cooling were performed with cooling by a combination of downward gravity driven water film flow and upward natural convection of air flow at the outer wall. During the tests, the steam generating power and water film flow rate were varied. Tests were conducted to examine the effect of water film flow at the outer surface and the effect of power, i.e., heat flux, variation. In this part of the tests, instrumentation to measure containment wall inner and outer temperatures, water film temperature and air temperature, water film flow rate, steam condensing rate in the containment, air velocity, and humidity of the ambient atmosphere was provided.

Fig. 9 shows the temperature profiles of the inner and the outer wall, water film, and air under the conditions of 7.4 kW/m^2 heat flux and 0.167 kg/s water film flow rate. As in the figure of the previous section, the abscissa represents the dimensionless distance from the top to the bottom along the wall. As

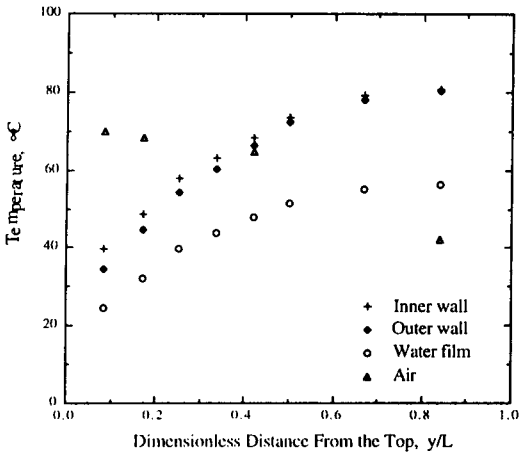

Fig. 9. Various Temperature Profiles Under the Conditions of 7.4 kW/m² Heat Flux and 0.167 kg/s Water Film Flow Rate

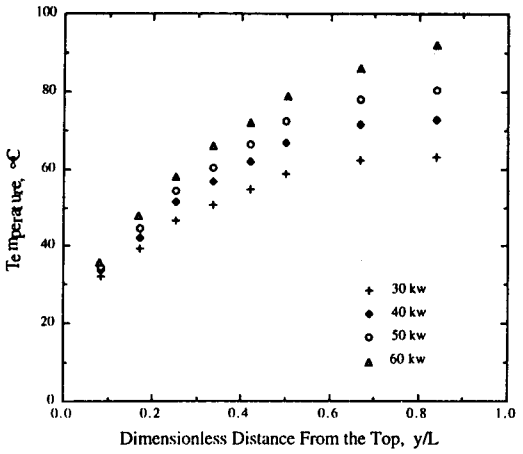

Fig. 11. Temperature Profiles of Outer Wall Surface at 0.167 kg/s Water Film Flow Rate for Various Power

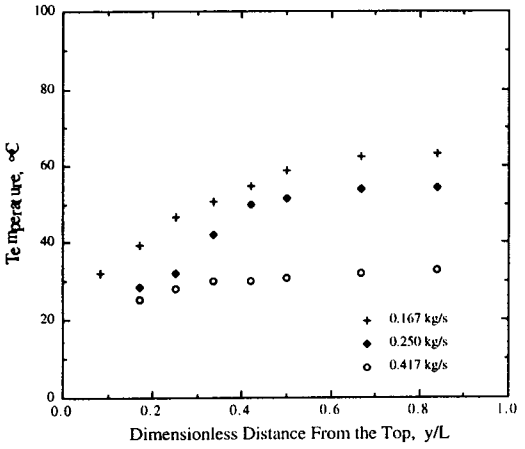

Fig. 10. Temperature Profiles of Outer Wall Surface at 4.45 kW/m² Heat Flux for Various Water Film Flow Rate

seen in this figure, water film flow causes a significantly lower tempeature distribution on the containment wall compared with cooling by only air natural convection. Therefore, containment cooling by water film flow at the outer wall is very effective to maintain the integrity of the containment structures during a postulated accident. Fig. 10 illustrates the influence of water film flow rate on the outer wall temperature distribution. The results show that the wall temperature decreases with increasing water film flow rate. Fig. 11 shows the effect of steam generating power on the outer wall temperature distribution for the constant water film flow rate. It indicates that the outer wall temperature increases with increasing steam generating power.

Heat transfer behaviour at the outer surface of the containment wall is somewhat complex because it is influenced by the combined effect of the convective and evaporative heat transfer processes. Fig. 12 shows the heat transfer coefficients at the inner and outer wall and the overall heat transfer coefficients under the condition of 7.46 kW/m² heat flux and 0.167 kg/s water film flow rate. The condensate and convective heat transfer coefficients were calculated with measured temperature data. The convective heat transfer coefficient with water film flow was based on the water temperature. It was assumed that the heat flux was uniform over the containment wall. As seen in Fig. 12, higher heat transfer rate can be observed

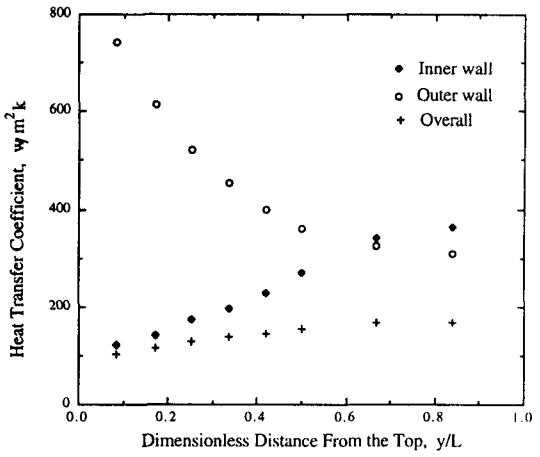

Fig. 12. Various Heat Transfer Coefficients at 7.46 kW/m² Heat Flux and 0.167 kg/s Water Film Flow Rate

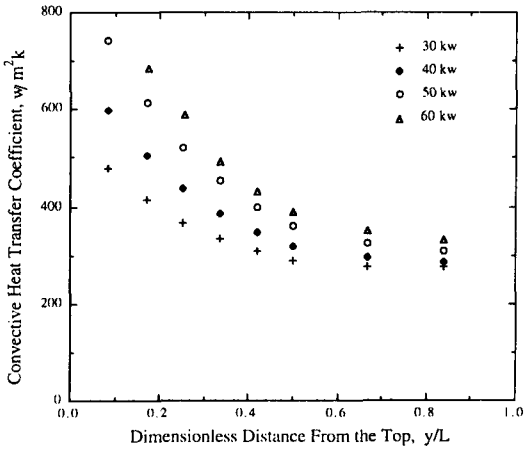

Fig. 13. Profiles of Outer Wall Heat Transfer Coefficients for Various Power at 0.167 kg/s Water Film Flow Rate

at the top part of the containment dome. Fig. 13 shows the plots of distribution of outer wall heat transfer coefficients for various steam generation power sizes. The outer wall heat transfer coefficient inclreases as power increases.

The measured average film coefficients at the outer wall are compared with Shmerler's correlation[9] for evaporative heating of a free-falling liquid films, Fujita's correlation[10] for highly subcooled free-falling water films, and Colburn's correlation[11] for forced convection heat transfer as shown in Fig. 14. As seen in this figure, present data are close on the Colburn's correlation. Colburn's correlation is expressed as:

$$Nu = 0.023\, Re^{0.8} Pr^{0.33} \quad (4)$$

where Nu is Nusselt number based on water, Re is Reynolds number based on water flow, and Pr is Prandtl number of water. In the above calculations, Reynolds number is defined as:

$$Re = \frac{4\gamma}{\mu} \quad (5)$$

where γ is water film flow rate per unit periphery

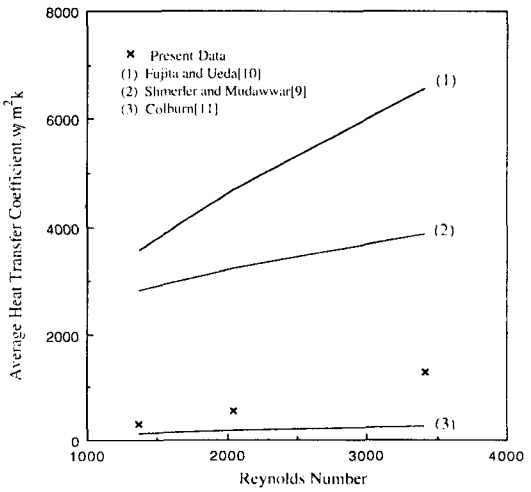

Fig. 14.. Comparison of Present Data and Other Correlations

and μ is viscosity of water. The measured data are still somewhat higher than Colburn's correlation. This may be attributed to the combined effects of convective and evaporative heat transfer processes.

Table 2 is the percentage of the dissipated heat

Table 2. Heat Balance of the PCC Tests

Power (kW)	Water Flow Rate (kg/s)	Q_1(%)	Q_2(%)	Q_3(%)
10	0.167	97.5	2.5	~ 0
20	0.167	86.0	1.9	12.1
30	0.167	81.3	1.5	17.2
40	0.167	72.3	1.7	25.6
50	0.167	64.1	1.1	34.8

from the outer wall of the containment with various heat transfer mediums. Where Q_1 is percentage of heat transferred by water film flow, Q_2 is percentage of heat transferred by air, and Q_3 is percentage of heat transferred through the air flow baffle wall. As seen in the table, the majority of heat was transferred by the water film. The heat transferred through the air flow baffle plate increased with power increasing.

4. Conclusions

The tests to find the heat transfer capability of the passive containment cooling system at the medium heat flux level were carried out. The following conclusions can be drawn from the test results:

(1) The natural convective heat transfer from the containment to the air without water film flow exceeded the expected values.

(2) There is a maximum heat flux that could maintain the state of equilibrium between condensation heat transfer at the inner wall and natural convection heat transfer by air at the outer wall. This maximum heat flux was 1.48 kW/m^2 in this test.

(3) No significant effect of the air flow baffle on air natural convection at the outer containment wall was observed during the test.

(4) Water film flow causes a significant low temperature distribution on the containment wall compared with cooling by only air natural convection. Therefore, water film flow for the containment cooling is very effective in maintaining the integrity of the structures of the containment during a postulated accident.

(5) The local heat transfer coefficient at the shoulder part of the ellipsoidal dome was higher than the vessel average heat transfer coefficient.

References

1. S.N. Tower, T.L. Schulz and R.P. Vijuk, Passive and Simplified System Features for the Advanced Westinghouse 600 MWe PWR, *Nuclear Engineering and Design*, Vol. 109, pp. 147~154, 1988.
2. T.V. De Venne, E. Piplica, M. Kennedy and J. Woodcock, The Westinghouse AP 600 Passive Containment Cooling *Test Analysis Program*, *Proceedings of the International Conference on Design and Safety of Advanced Nuclear Power Plants*, Tokyo, October 25−29, pp. 17. 1−1~8, 1992
3. W.A. Carbiener and R.A. Cudnik, Similitude Consideration for Modelling Nuclear Reactor Blowdown, *Trans.* ANS, Vol. 12, p. 361, 1969.
4. W. Nusselt, Die Oberflachenkondensation des Wasserdampfes, *VDIZ.*, Vol. 60, p. 541, 1916.
5. G. Hugot, Etude de la Convection Naturelle Entre Deux Plaques Planes, Verticales, Paralleles et Isothermes, Doctoral Dissertation, University of Paris, 1972.
6. J.J. Shin, R.C. Lotti, and R.F. Wright, NPR and ANS Containment Study Using Passive Cooling Techniques, *Proceedings of the 8th KAIF/KNS/OKAEA Annual Conference*, Seoul, pp. 91−99, 1993.

7. S.W. Churchill and H.S. Chu, Correlation Equations for Laminar and Turbulence Free Convection from a Vertical Plate, *Int. J. Heat Mass Transfer*, Vol. 18, p. 1323, 1975.
8. E.M. Sparrow, P.C. Stryker, and M.A. Ansari, Natural Convection in Inclosures with Off Center Innerbodies, *Int. J. Heat Mass Transfer*, Vol. 27, pp. 49~56, 1984.
9. J.A. Shmerler and I. Mudawwar, Local Evaporative Heat Transfer Coefficient in Turbulent Free-Falling Liquid Films, *Int. J. Heat Mass Transfer*, Vol. 31, pp. 731~742, 1988.
10. T. Fujita and T. Ueda, Heat Transfer to Falling Liquid Films and Film Breakdown, *Int. J. Heat Mass Transfer*, Vol. 31, pp. 67~77, 1978.
11. A.P. Colburn, A Method of Correlating Forced Convection Heat Transfer Data and a Comparison with Fluid Friction, *Trans. Am. Inst. Chem. Engrs.*, Vol. 29, p. 174, 1933.